WANG, S., TAKYI-ANINAKWA, P., JIN, S., LIU, K. and FERNANDEZ, C. 2023. An improved sliding window: long short-term memory modeling method for real-world capacity estimation of lithium-ion batteries considering strong random charging characteristics. *Journal of energy storage* [online], 70, article 108038. Available from: https://doi.org/10.1016/j.est.2023.108038

An improved sliding window: long short-term memory modeling method for real-world capacity estimation of lithium-ion batteries considering strong random charging characteristics.

WANG, S., TAKYI-ANINAKWA, P., JIN, S., LIU, K. and FERNANDEZ, C.

2023

An improved sliding window - long short-term memory modeling method for real-world capacity estimation of lithium-ion batteries considering strong random charging characteristics

Shunli Wang[1, 2*], Paul Takyi-Aninakwa[2], Siyu Jin[3], Ke Liu[2], Carlos Fernandez[4]

[1] College of Electrical Engineering, Sichuan University, Chengdu 610065, China; [2] School of Information Engineering, Southwest University of Science and Technology, Mianyang 621010, China; [3] Department of Energy Technology, Aalborg University, Pontoppidanstraede 111 9220 Aalborg East, Denmark; [4] School of Pharmacy and Life Sciences, Robert Gordon University, Aberdeen AB10-7GJ, UK.

Abstract: Capacity estimation plays a significant role in ensuring safe and acceptable energy delivery, especially under real-time complex working conditions for whole-life-cycle lithium-ion batteries. For high-precision and robust capacity estimation, an improved sliding window-long short-term memory (SW-LSTM) modeling method is proposed by introducing multiple time-scale charging characteristic factors. The optimized feature information set is extracted by constructing an optimized differential integration-moving average autoregressive (DI-MAA) model, which is introduced as the input matrices of the whole-life-cycle capacity estimation model. With the constructed DI-MAA model, the relevant features are effectively extracted, overcoming the data limitation problem of the long-term dependence capacity estimation. For the experimental test, the maximum capacity estimation error is 3.56%, and the average relative error is 0.032 under the complex Beijing bus dynamic stress test working condition. The proposed SW-LSTM estimation model with optimized DI-MAA-based data pre-processing treatment has high stability and robust advantages, serving an effective safety assurance for lithium-ion batteries with real-world complex working condition adaptation advantages.

Keywords: lithium-ion battery; sliding window - long short-term memory; capacity estimation; differential integration - moving average autoregressive model; multiple time-scale factors

***Corresponding author:** Shunli Wang. E-mail address: wangshunli1985@qq.com.

Highlights:

- An improved SW-LSTM model is constructed for real-time capacity estimation

- The optimized DI-MAA strategy is formed for feature extraction and data pre-processing
- The high-accuracy results are obtained with the real-world capacity estimation error of 3.56%
- The proposed model has high stability and accuracy for real-world capacity estimation

1. Introduction

With the advantages of fast charging ability, high energy density, low self-discharge rate, no memory effect, and a long lifespan, lithium-ion batteries are widely used in new energy vehicles (EVs), communication facilities, electrical equipment in aeronautics, smart devices such as mobile phones, laptops, grids, etc. [1, 2]. However, the battery's capacity performance decreases inevitably along with an increasing number of charge-discharge cycles, which results in capacity and power fade in addition to electrochemical instabilities causing thermal runaways and fire accidents. Consequently, accurate capacity estimation by the battery management systems (BMS) is not only crucial for the safety assurance of lithium-ion batteries but also plays a significant role in the real-time application of EVs [3-5].

Most of the capacity estimation methods are limited by the length of the training data, which cannot adapt to robust real-world applications. Also, their value is difficult to estimate accurately when the testing and training datasets are different under various working conditions [6-8]. Many battery-based industrial applications suffer from a lack of maintenance, adverse working conditions, and poor operation, which leads to an accelerated battery degradation process. It is the reason why online capacity estimation is becoming a hot research topic [9-12]. Using the dynamic impedance changes can realize the capacity estimation purpose, including the model-based and data-driven methods. The data-driven methods do not need to establish a specific battery model based on the complex electrochemical and degradation mechanisms [13-17]. Only the monitoring data is used in the cyclic charge-discharge processes to fit the degradation law of battery performance, which is more universal than the model-based methods. To realize reliable energy and safety management, high-precision capacity estimation plays an important role in the BMS along with the battery system application.

Along with the development of cloud computing, data-driven methods are becoming increasingly attractive for online capacity estimation. However, existing data-driven methods still have low accuracy and weak robustness [18]. Due to the characteristics of capacity regeneration, nonlinearity, and random fluctuation of lithium-ion batteries, the generalization ability is poor when only a single-scale feature is used to realize the capacity estimation. Consequently, the convolutional neural network (CNN) is introduced into the degradation model as an effective deep learning (DL) method. It realizes capacity estimation using sparse data segmentation through cloud computing and extracts hidden feature information of different depths effectively [19-21]. The hybrid validation dataset-based induced order weight geometric averaging operator is also constructed to precisely capture the extracted features, which are related to the health status and remaining useful life (RUL) of lithium-ion batteries based on a variant long short-term memory (LSTM) neural network [22]. The data-driven support vector machine (SVM), LSTM network, and Gaussian process regression are introduced to realize the capacity estimation with the support of the extracted health features. The spatiotemporal relationships are extracted using the random forest algorithm to capture nonlinear characteristics for multi-step-ahead capacity estimation [22-27]. The hybrid model based on an attention mechanism and bidirectional (Bi) LSTM model is established for the RUL prediction using whole-life-cycle datasets [28], constructing new hidden layer discarding techniques. This modeling strategy prevents the model overfitting phenomenon and enables accurate RUL prediction based on capacity traction combined with soft perception, accommodating local regeneration and fluctuations [29-31]. The deep domain adversarial networks are constructed with an unsupervised feature alignment metric by considering the maximum mean discrepancy and correlation alignment [32]. However, due to insufficient data pre-processing, the model is disturbed by the noise component of the original input data [33, 34]. With the continuous enhancement of artificial intelligence algorithms, the deep learning theory has been gradually popularized and applied, especially the LSTM-based model construction concept, which has become a significant methodology for the capacity estimation of lithium-ion batteries.

Due to the enhanced capabilities of the LSTM network and other modeling methods, they have been constructed to improve the accuracy of capacity estimation for lithium-ion batteries [35-37]. The LSTM network performs well at time series estimation, which is used to establish a capacity estimation framework. A controllable deep transfer learning (CDTL) model is constructed for the short- and long-term charge state estimations at early stages of degradation based on improved

LSTM architectures, making it have better generalization ability in the estimation process under different stress conditions [38]. A hybrid approach for online cycle lifetime estimation has been proposed by combining a Bi-LSTM model with the attention mechanism (Bi-LSTM-AM) in comparison to a support vector regression (SVR) model [39]. The proposed method is based on the initial temperature data measured online, which is updated using the SVR model to obtain advanced multi-step temperature estimation. Then, the Bi-LSTM-AM model is constructed to predict the cycle life status. Parallel attention networks are constructed by combining multivariate time series to extract the relationship between the selected health features and the state of health (SOH) factor [40, 41]. Finally, a novel parallel learning framework is constructed by integrating an attention mechanism and the LSTM network, which can fully utilize the health features and help to solve the challenging issues of estimation accuracy and robustness [42]. Combining the characteristics using an adaptive gated recurrent unit (GRU), a DL-based RUL prediction network is constructed to describe the uncertainty of estimation results through a Monte Carlo optimization. An integrated capacity estimation method is proposed by conducting the local tangent space alignment (LTSA) feature extraction and adaptive sliding window (ASW)-LSTM model [43]. The indirect health indicator (HI) is extracted automatically by the LTSA to replace the immeasurable capacity. Then, its strong correlation is verified by the Spearman correlation coefficient. For high-precision capacity estimation, multiple optimization strategies are proposed with the LSTM-based main modeling structure that is suitable for whole-life-cycle capacity estimation.

To improve model accuracy, an improved LSTM-RNN model is employed to express the long-term dependencies among the degraded capacities of lithium-ion batteries. Consequently, the procedure is optimized adaptively using the resilient mean square backpropagation calculation and the dropout technique [44]. DL-based prognostic methods are introduced with online validation, according to which the effective variety of RNNs with the LSTM architecture is constructed with variable input dimensions that facilitate the network training process with additional labeled samples [45-47]. An attention-based RNN model is constructed to improve the prognostics and health management effect, which enables a more accurate estimation of output voltage degradation using the original long-term dynamic cycle durability test data [48]. In contrast, the DL-based method is easy to operate, overcoming the whole-life cycle capacity estimation problem effectively [49-52]. Higher intercycle aging resolutions are realized for faster and more accurate estimation by considering the temporal patterns and cross-data correlations in the raw data of terminal voltage, current, and cell temperature [53-58]. Considering the whole-life-cycle characteristics of battery-based energy supply conditions, lots of inner and outer factors should be considered in the iterative calculation processes.

In the present DL-based capacity estimation methods, the whole-life-cycle information effect on multiple inner-state factors is not considered comprehensively. Therefore, by considering the internal parameter coupling mechanism of capacity, impedance, and temperature, this paper presents an improved sliding window-long short-term memory (SW-LSTM) model for accurate cycle-to-cycle capacity estimation, which is adaptive to complex working conditions for lithium-ion batteries. In the proposed SW-LSTM-based iterative calculation and capacity estimation process, an optimized differential integration - moving average autoregressive (DI-MAA) modeling strategy is introduced for feature extension to realize the feature information optimization and optimize the historical data together with the estimation models of formulations, improving the estimation accuracy even despite short-term test data containing insufficient global degradation information. The optimized iterative calculation strategy is introduced into the capacity estimation process and characterizes the degradation patterns simultaneously through uncertainty estimation and variational inference, improving the capacity estimation effect and fault diagnosis performance for high-efficiency predictive maintenance.

The remaining sections of this article are organized as follows: Section 2 is the mathematical analysis, in which the proposed improved SW-LSTM model and the established DI-MAA modeling strategy for feature extraction and optimization are described. Section 3 presents the experimental battery tests, the capacity estimation, and the validation results. Finally, the conclusion and future research plans are presented in Section 4.

2. Mathematical analysis

2.1. Upgraded sliding window - long short-term memory modeling framework

The improved SW-LSTM model is constructed, the framework of which involves three main stages for achieving the capacity estimation objectives. (1) The charging capacity is selected as the health factor innovatively, reflecting the degradation trend for the cycle-to-cycle capacity estimation. In the real-world application process, it is easier to measure the charging capacity with the constant current-constant voltage (CC-CV) charging process than with the complex varying current in the discharging process. Also, to make the result more accurate, the fluctuation caused by the capacity recovery phenomenon in the original data is removed by using the adaptive sliding window method with smoothing techniques. Then, the capacity series is obtained from a relatively stable degradation trend. (2) Using the smoothed capacity sequence, the residual and finite modal components are extracted to reflect the main degradation trend. (3) The residuals are extracted to form the training dataset, which is combined with the LSTM network to establish the mapping relationship between early and late capacities to estimate the unknown capacity series. According to this designed framework, the cycle-to-cycle capacity is estimated during the iterative calculation process after the starting point is determined.

The features of the real-world parameters are considered to express the aging characteristics, mainly including current magnification, SOC, temperature, and other parameters. Then, the processing model is constructed accordingly to reflect the influence of the operating conditions effectively, realizing the weight coefficient preset effectively. Considering the instantaneous voltage drop and the degradation processes that occur when the load current is formed, the variation law is explored to obtain the influencing factors of internal ohmic resistance and polarization effects. Then, it is combined with the phased expression of instantaneous voltage rise, deceleration, and stabilization after the current interruption. With the concept of pre-processing treatment for state evaluation, the iterative calculation and correction procedure of the SW-LSTM model is constructed for the cycle-to-cycle capacity estimation, as shown in Figure 1.

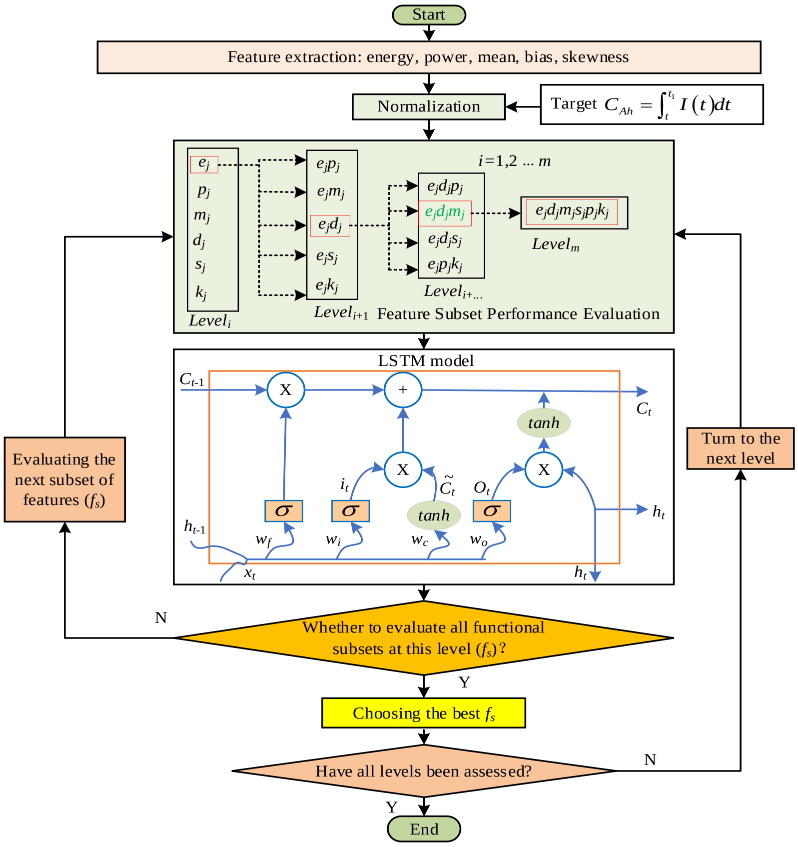

Figure 1. Capacity correction and estimation based on the SW-LSTM model

In Figure 1, the original input data are normalized firstly. Then, the optimized feature subset performance evaluation is extracted as the input of the LSTM model by introducing the sliding window smoothing strategy. When all functional subsets are evaluated by levels, the best output is obtained. Exceptionally, the cell-to-cell LSTM estimation model is an improved version of the recurrent neural network (RNN), which is introduced to eliminate the gradient vanishing and explosion problems during the backpropagation through time to retain the ability of the network to solve long sequence dependence prediction [59, 60]. The key element of LSTM is the memory cell, which is at the center of each linearly activated neuron. It can be thought of as a channel for the addition of new information or the removal of some information. Using "gates" and other structures in this process, the flow of information is successfully handled [61].

The status of the memory cell is saved and controlled through three determined gates, including the forget gate, the input gate, and the output gate, which are expressed by f_t, i_t, and o_t, respectively. The forget gate is used to decide what information should be discarded from the cell state in the capacity estimation process, as shown in Equation (1).

$$f_t = \sigma\left(W_{fh}\square_{t-1} + W_{fx}x_t + b_f\right) \tag{1}$$

In Equation (1), f_t is the output of the forget gate; σ is the sigmoid function; W_{fh} and W_{fx} are the weight matrices of the forget gate used for the training of the network. $\square_{t-1}$ is the median hidden state of the output gate for the present LSTM unit; x_t is the input of the neuron at time point t and b_f is the bias vector of the network. Similarly, the input gate is constructed to output the computational calculation result of the sigmoid and the hyperbolic tangent functions to the next layer. The mathematical calculation processes of the input gate and the memory cell are shown in Equation (2).

$$\begin{cases} i_t = \sigma(W_{ih}\square_{t-1} + W_{ix}x_t + b_i) \\ \tilde{C}_t = tanh(W_{ch}\square_{t-1} + W_{cx}x_t + b_c) \end{cases} \tag{2}$$

In Equation (2), i_t is the input gate; σ is the sigmoid function; W_{ih} and W_{ix} are the weight matrices attached to the input gate during the training of the network; $\square_{t-1}$ is the median hidden state of the present LSTM unit. b_i and b_c are the bias vectors for the input gate and cell memory, respectively; $\tilde{C}_t$ is the call state at the present time point; $tanh$ is the hyperbolic tangent function; W_{ch} and W_{cx} are the weight matrices attached to the memory cell during the update of the current relevant information that needs to be stored in it. Finally, the output layer is constructed to update the old cell state to the new cell state, as shown in Equation (3).

$$\begin{cases} C_t = f_t C_{t-1} + i_t \tilde{C}_t \\ o_t = \sigma(W_o\square_{t-1} + W_o x_t + b_o) \\ \square_t = o_t \cdot tanh(C_t) \end{cases} \tag{3}$$

In Equation (3), C_t is the cell state information at the present time point; f_t is the forget gate and the functional relationship $(\cdot)$ is the Hadamard point-by-point multi-application component. C_{t-1} is the memory state at the last time point. i_t is the input gate. $\tilde{C}_t$ is the cell state factor of the neuron state at the present point and o_t is the information of the output gate. W_o is the weighting matrix for the output gate after the training process. $\square_{t-1}$ is the output of the hidden layer for the previous time point $t-1$. b_o is the bias vector of the output gate. $\square_t$ is the output of the hidden layer for the previous time point t.

In the proposed SW-LSTM model, the learning ability of the long-order dataset treatment is greatly improved with front and back dependencies by considering the learning effects, which include past and future states on the current capacity state parameters simultaneously. With this treatment, the disadvantages in the training and testing processes, including only studying the impact of past state factors on current state factors, are effectively overcome for the LSTM network, by ignoring the role of future states. Also, the inefficient use of the pre-dependence and post-dependence of time series is retarded, as it is the limited ability of data learning. The improved SW-LSTM network can benefit from the time-series data independently through the recurring process in the step-by-step gating layers. The feed-forward processing results from the input and forget layers are introduced into the output layer simultaneously, which can make full use of the life information contained in the past and future time data sequences.

In the form of cyclic iteration for the pre-treatment to the evaluation and prediction steps, the model parameters, state variables, and variance are modified in real-time to improve the accuracy of the capacity estimation, which is used to enhance the model's adaptability under complex working conditions. When the noise is unknown, the internal resistance is estimated by controlling the error range to improve stability and convergence in the capacity estimation process. The LSTM-RNN-based estimation network is constructed for feature optimization, as shown in Figure 2.

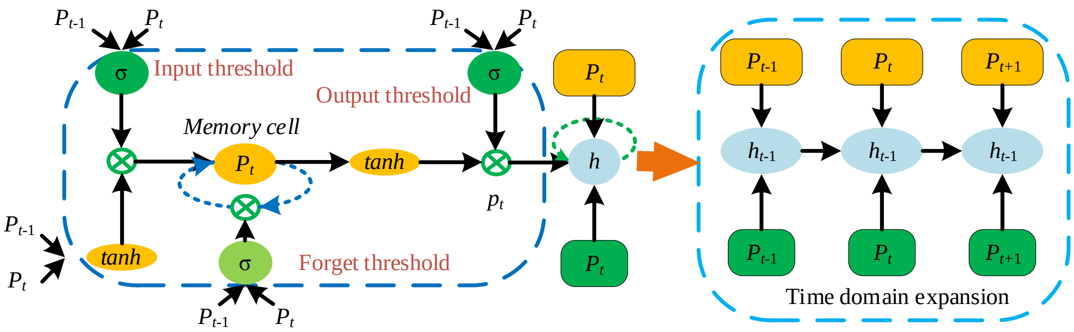

Figure 2. Construction of the LSTM-RNN-based estimation network for feature optimization

In Figure 2, based on the constructed LSTM-RNN estimation network framework, the capacity is calculated synchronously to ensure the modeling accuracy. The optimized structure for the time domain expansion is introduced to improve the accuracy of the estimation results, according to which the computational complexity is effectively reduced for the characterization process. As the estimation accuracy is limited by the current time stage, the data provided by the measurement system in the early stages is also limited, including the parameters of current, voltage, and temperature. Therefore, it is relatively difficult to deeply explore the implicit relationship between aging inducement, multi-parameter estimation, and cycle life during the capacity estimation process. Over time, the data scale and quality available for the network's training set are supposed to increase gradually by flowing through the constructed LSTM-RNN framework, which improves the capacity estimation accuracy synchronously. To solve the RNN-based gradient explosion or disappearance problems, the LSTM-based network is introduced into the calculation procedure, in which the state unit of the RNN is replaced by the cyclic unit structure of the LSTM network. When constructing the LSTM-RNN-based estimation model, the structural bi-directional design is considered for the input, output, and hidden layers, as well as the training and estimation of the network, including the forward direction and backward direction computation processes, as shown in Figure 3.

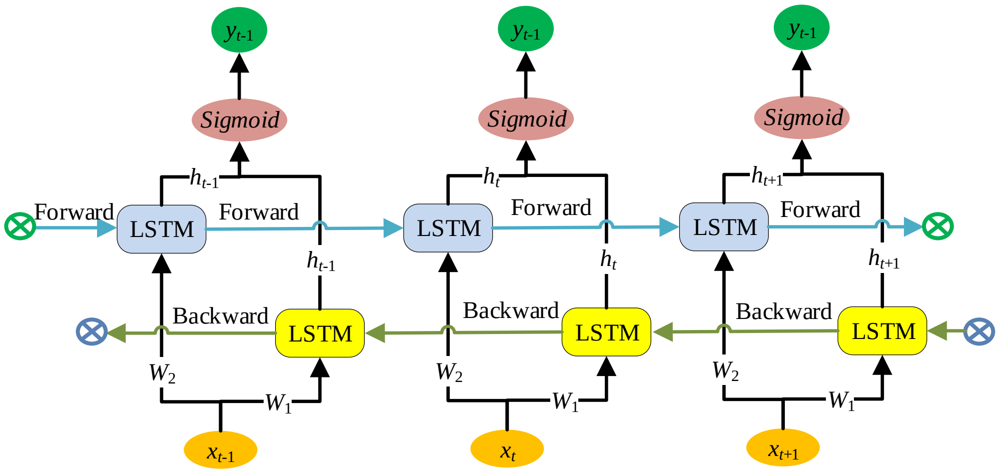

Figure 3. An illustrative framework of the power battery for time series estimation based on LSTM-RNN

In Figure 3, each gate in the network has a weight W_f, W_i, W_c, and W_o associated with the forget gate, input gate, memory cell, and output gate, respectively. Also, the network possesses a bias b_f, b_i, b_c, and b_o vector attached to each gate. This pre-treatment is conducted to enhance the network flexibility and make it adaptive to the training data for accurate battery characterization by filtering out the observation noise and process noise, which are affected by environmental conditions and restricted by the computing power of BMS processors. The main structure of the optimized bidirectional SW-LSTM model is constructed by the combination of two unidirectional recurrent networks, in which the inputs are the same, and the information is transmitted in opposite directions with symmetrical structures. Correspondingly, the multiple LSTM components are introduced to extract the bidirectional spatiotemporal feature information, as shown in Equation (4).

$$\begin{cases} h'_t = f(W_1 x_t + W_3 h'_{t-1} + b'_t) \\ h_t = f(W_2 x_t + W_4 h_{t-1} + b_t) \\ H_t = h'_t \oplus h_t \end{cases} \tag{4}$$

In Equation (4), h'_t is the hidden layer state output, h_t is the hidden layer state information, f is the activation function of the hidden layer, and $\oplus$ is the vector concatenation operator.

To eliminate the influence of the measurement unit and its magnitude in the input data for the vector of current, voltage, and temperature, it is normalized to improve the robustness, convergence rate, and acceleration of the gradient descent for the LSTM network. Specifically, before the input data are introduced into the LSTM network for real-time capacity estimation and iterative calculation, [-1, 1] is used to normalize the index data, including voltage, current, temperature, and SOC, as shown in Equation (5).

$$x_{nom} = \frac{2(x - x_{min})}{x_{max} - x_{min}} - 1 \tag{5}$$

In Equation (5), x_{nom} is the normalized data and x is the original data for the input vector of current, voltage and temperature. x_{max} is the maximum value in the original data. x_{min} is the minimum value in the original data.

In the early estimation stage, a multivariate hidden Markov model (HMM) is constructed to conduct a multi-factor real-time weighted correlation of aging incentives, state parameters, and rated capacity to achieve accurate short-term SOC estimation and error correction, which is also used as one input parameter for the real-time capacity estimation. In the latter estimation process, combined with the LSTM-RNN network framework, the improved dual feedback correction mechanism of features and time series is introduced to conduct the capacity estimation considering both the long-term and short-term memory time series. The correlation and time dependence are used to improve the estimation accuracy. The correlation relationship is extracted between characteristic parameters, environmental conditions, and operation data. After that, the real-time correction of auxiliary information is realized by independently optimizing key time points and enhancing mathematical expressions, which is used to improve the estimation effect and stability over a long period.

2.2. *Differential integration - moving average autoregressive modeling method*

The LSTM component only considers the influence of past states on current states by ignoring the role of future state parameters, so it does not consider the pre- and post-dependent time series problem and has a limited ability to learn the data information. The proposed SW-LSTM model learns the effects of past and future states on the current state simultaneously, which greatly improves the learning ability of the model for long-order data with front and rear dependencies. The DI-MAA model is constructed to process the time series data independently through the forward and backward layers, which feed the processing results of the two layers to the output layer. Consequently, it can make full use of the life information contained in the past and future time sequence data. By constructing the deep neural network with a recursive architecture, the higher-level data features are extracted from the original data. With the existence of the gate structure, the DI-MAA model can judge and screen the past information flow itself. Then, the full learning of the training set is completed. Finally, the nonlinear mapping relationship between the early and later stages of capacity is established. The unreasonable interval in the original capacity series is eliminated. The program operation has little correlation with the amount of data, so the execution time is constant.

With the DI-MAA pre-processing of the measured datasets, the SW-LSTM-based capacity estimation model has a strong learning ability for time series data and can achieve higher accuracy. The result of the model is interval estimation rather than point-to-point, which reflects the uncertainty. After the DI-MAA-based data treatment, the SW-LSTM model is introduced into the model to describe the uncertainty of the estimation results. The parameters of the SW-LSTM model are regarded as random variables subject to a certain distribution, in which X represents the training dataset and Y represents the corresponding real capacity value. As for the nonlinear characteristics of the lithium-ion batteries, the sliding time window is constructed to extract the new feature of the measured dataset, which is then introduced into the SW-LSTM model as an input, and the DI-MAA-based pre-processing architecture is designed, as shown in Figure 4.

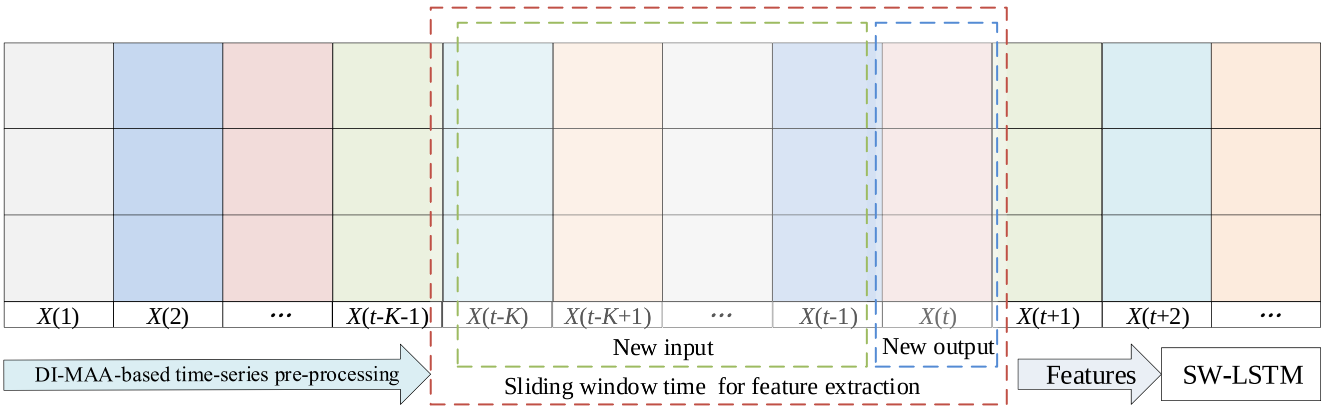

Figure 4. The DI-MAA-based new dataset construction process for the input pre-processing of the SW-LSTM model

In Figure 4, the dataset is pre-processed using the DI-MAA-based pre-processing architecture as well as the fixed sliding window with a window length of $K-1$. The first data sequence from $X(t-K)$ to $X(t-1)$ in the processing window is used as the input of the SW-LSTM model. The last data vector is taken as the corresponding output. Using the sliding window, multiple sets of features are extracted for the input and output data sequences. It reduces the role of irrelevant parts by designing various weighting coefficients for different calculation parts. This " many-to-one" structure can improve the utilization ability of the estimation model for the historical discharge data. Even if the discharge data at different historical times in the input sample have different effects on the current state parameters, they are equally treated using this modeling structure effectively. Therefore, to improve the filtering effect of the window data as model input, an effective attention mechanism is designed to make the model give priority to the discharge data that has a great impact on the current state parameters. Consequently, it further improves capacity estimation accuracy, which is adaptive to complex working conditions. The steps of the attention mechanism are designed accordingly.

Firstly, a scoring function is used to calculate the correlation score of the eigenvector between $h_{t,i}$ and h_t for the discharge data at each time in the hidden state. This step is realized by a full connection layer with the number of output nodes τ, and its input is the hidden state h_t^T after transposition, as shown in Equation (6).

$$score([h_{t,i}, h_t]) = \mathrm{W}_s h_t^T + b_s \tag{6}$$

In Equation (6), W_s is the weight matrix and b_s is the bias vector of the full connection layer. $score([h_{t,i}, h_t])$ is the relevant information between $h_{t,i}$ and h_t. Then, the attention weight α_i of each time input data in the sample is obtained by using the softmax function. Its weighted aggregation with $h_{t,i}$ is used to obtain the output h_t^* of the attention layer, as shown in Equation (7).

$$\begin{cases} \alpha_i = \dfrac{exp\{score([, h_t])\}}{\sum_{j=1}^{\tau} exp\{score([h_{t,i}, h_t])\}} \\ h_t^* = \sum_{j=1}^{\tau} \alpha_i h_{t,i} \end{cases} \tag{7}$$

Finally, h_t^* is input into the full connection layer with one output node, obtaining the estimation value of the state factor, as shown in Equation (8).

$$\hat{y}_t = W h_t^* + b \tag{8}$$

In Equation (8), W is the weight matrix of the full connection layer, and b is the bias vector. The random variable $\theta = \{W, b\}$ is constructed to represent the model parameters. Considering the complexity of calculating the key divergence when there are many neurons, the objective function is optimized under the L2 regularization condition using the equivalence between the dropout layer and Bayesian variational inference, as shown in Equation (9).

$$L_{dropout} = \frac{1}{p}\sum_{t\in S} E(Y, \hat{Y}) + \sum_{h=1}^{H} [\lambda \|W\|^2 + \lambda \|b\|^2] \tag{9}$$

In Equation (9), S is the subset of training samples and p is the number of subsets. H is the total number of model parameters, $\hat{Y}$ is the model output obtained by dropout, and λ is the attenuation coefficient of regularization. This objective function is optimized using the adaptive moment estimate (ADAM) optimizer. When the optimal approximate distribution of the posterior distribution of the model parameters is obtained, the distribution of the model capacity estimation results for the newly obtained input sample X^* is extracted, as shown in Equation (10).

$$p(Y_t^* | X_t^*, X, Y) = \int p(Y_k^* | X_k^*, \theta) q^*(\theta)\, d\theta = \frac{1}{T}\sum_{t=1}^{T} p(Y^* | X^*, \hat{\theta}_t) \tag{10}$$

In Equation (10), $\hat{\theta}_t$ is the specific sampling value of $q^*(\theta)$, and T is the cyclic sampling number.

2.3. *Uncertainty quantification and evaluation criteria*

To evaluate the capacity estimation effect of the proposed SW-LSTM model, the mean absolute error (MAE), root mean square error (RMSE), mean absolute percentage error (MAPE), and R^2 (coefficient of determination) metrics are introduced for critical analysis in real-world applications, as shown in Equation (11).

$$\begin{cases} E_t = y_t - \hat{y}_t \\ MAE = \dfrac{1}{m}\sum_{t=1}^{m}|y_t - \hat{y}_t| \\ RMSE = \sqrt{\dfrac{1}{m}\sum_{t=1}^{m}(y_t - \hat{y}_t)^2} \\ MAPE = \dfrac{1}{m}\sum_{i=1}^{m}\left|\dfrac{y_t - \hat{y}_t}{y_t}\right| \\ R^2 = 1 - \dfrac{\sum_{t=1}^{N}(E_t)^2}{\sum_{t=1}^{N}(y_t - \bar{y})^2} \end{cases} \tag{11}$$

In Equation (11), m is the total number of data points. y_t represents the real capacity value of the lithium-ion batteries at the tth time point. $\hat{y}_t$ represents the estimated capacity value and $\bar{y}$ is the average value of the actual SOC of the model at the tth time point.

3. Experimental Section

3.1. *Experimental platform design*

The instruments include charge-discharge battery test equipment, a temperature chamber, and other supporting experimental equipment, providing a suitable and safe battery test environment. The experimental battery test platform is designed, as shown in Figure 5.

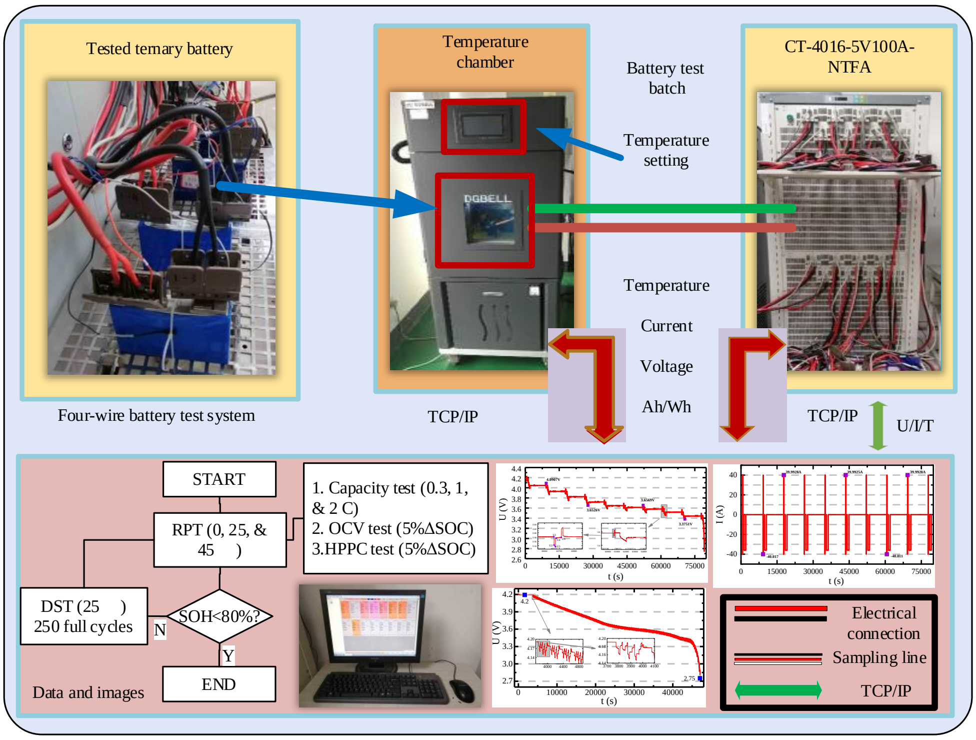

Figure 5. Experimental test platform for complex current-temperature working condition tests

In Figure 5, the experimental test procedure is designed and embedded in the host computer that is connected to the CT-4016-5V100A-NTFA charge-discharge battery tester using a TCP/IP channel. According to the platform design, the signals of U/I/T are measured accurately online. All the testing batteries are fixed in the chamber, according to which the time-varying current, voltage, and temperature variables under the test working conditions are constructed. As the model parameters vary along with the changing temperature, trials are conducted at an ambient temperature of 25 ℃. Meanwhile, the reference performance test is conducted at 0, 25, and 45 ℃ temperature conditions with a current rate of 0.3, 1, and 2 C. Then, the varying-temperature model parameters are further improved and applied in the iterative calculation process according to the complex working condition requirements.

3.2. *Capacity estimation effect and analysis*

The whole-life-cycle experimental test is conducted for the capacity estimation and verification effect of the proposed SW-LSTM model. The shared link of the original dataset is https://www.researchgate.net/project/Battery-life-test. It is the whole-life-cycle experimental data carried out by the research team members in the early stages. It is completed in cooperation for the whole year, even including the early-stage experimental design process and Origin graphing software. In this verification, the battery cell numbered 007 is selected, and the charging capacity recording dataset is introduced into the training and testing processes.

As for the whole-life-cycle variation in adaptive ability, the 20*25 = 500 cycling Beijing bus dynamic stress test (BBDST) experimental data are considered. During the application process, the discharging process is determined by the realistic application requirements, and only the parameters of the charging process are recorded. The charging capacity is used for the main variation analysis to make the proposed SW-LSTM model suitable for real-time application. The charging capacity is not only influenced by the aging process, but also influenced by working conditions and the environment, so it has a large and complex change, which will make the capacity estimation difficult, as shown in Figure 6.

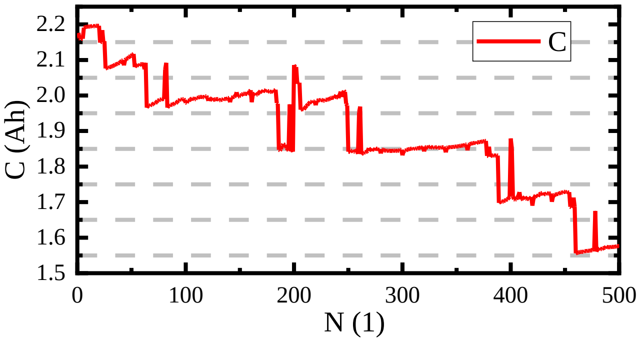

(a) Charging capacity variation curve

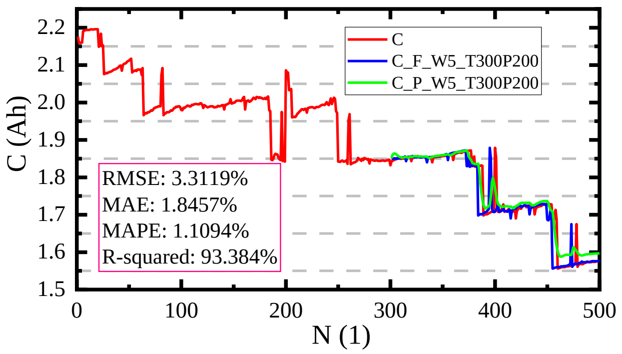

(b) Charging capacity estimation with W5_T300P200

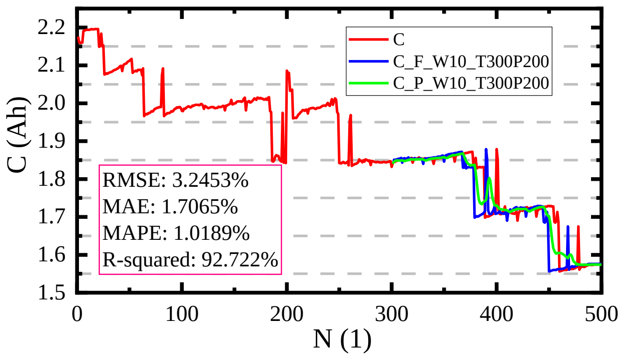

(c) Charging capacity estimation with W10_T300P200

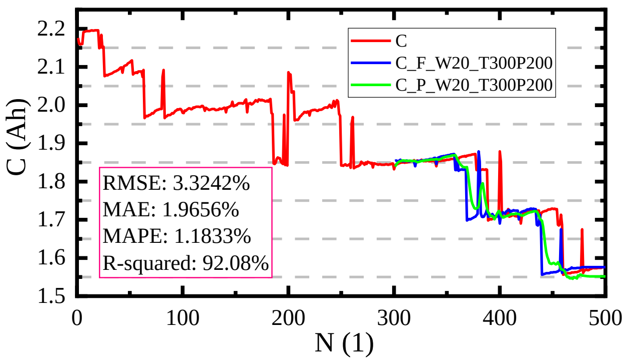

(d) Charging capacity estimation with W20_T300P200

Figure 6. Charging capacity variation and estimation curves with varying window length comparison under the real-world BBDST working conditions

In Figure 6, Wm is the window width of m, including 5, 10, and 20, and T_xP_y is the origination with a training dataset length of $x = 300$ and an estimation dataset of $y = 200$. Also, F and P denote filtering and predicting, respectively. For filtering, the dataset is directly used when measured by the sensors. For prediction, the capacity is estimated using the existing dataset from the previous time points after training the network. The blue and green curves represent the cycle-to-cycle capacity estimated by the SW-LSTM model, respectively. Compared with other window width values, these values have a better estimation effect. For the comparison of subfigures (b), (c), and (d), the $W10$ has an optimal estimation effect with an overall best RMSE value of 3.2453%, an MAE value of 1.7065%, a MAPE value of 1.0189%, and an R-squared value of 92.722% showing high adaptability and robustness in accurately estimating the capacity of lithium-ion batteries using this parameter value. Meanwhile, using a sliding window size of 20, it can be observed that the capacity estimate loses track of the actual capacity with high levels of fluctuation near the end of discharge. Using the RMSE, MAE, MAPE, and R-squared metric values for the charging capacity estimation by the proposed SW-LSTM model is shown in Figure 7.

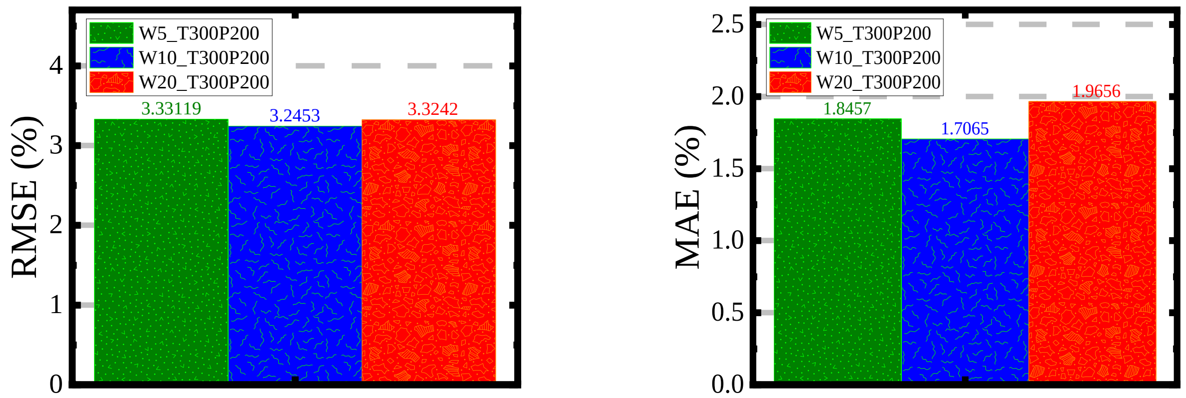

(a) RMSE histogram (b) MAE histogram

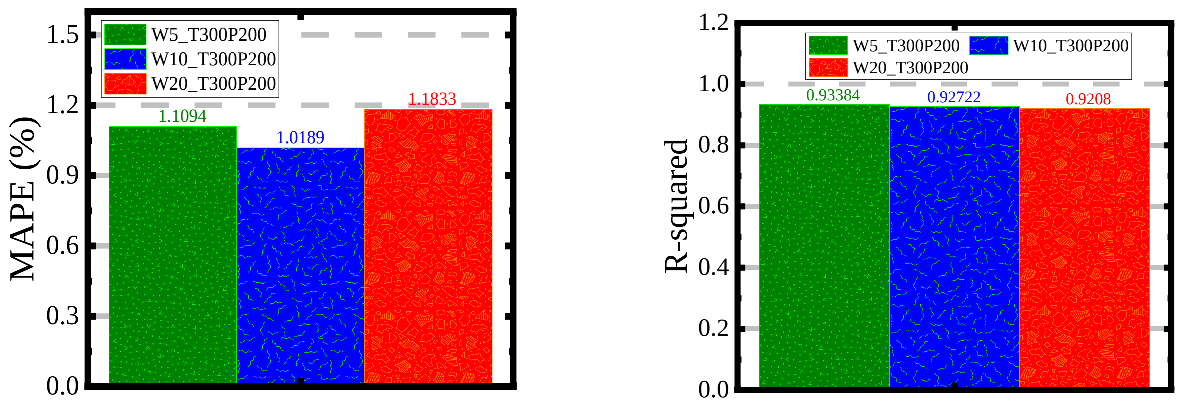

(c) MAPE histogram (d) R-squared histogram

Figure 7. Evaluation metric curves for different capacity estimations using different sliding window sizes

In Figure 7, compared with the estimation result using different sliding window sizes, it can be observed that the metric values of W10 are relatively optimal, and the charging condition capacity estimation of the battery is consistent. Its RMSE, MAE, MAPE, and R-squared values are 3.2453%, 1.7065%, 1.0189%, and 92.722%, respectively. The results of the proposed SW-LSTM estimation model show a high level of robustness, especially for these metrics when using different sliding window sizes at the same training and testing cycles.

3.3. *Varying training-estimation length adaptive analysis*

The charging capacity is affected by various uncertain factors in the working process, so the collected data contains a lot of noise and fluctuation. If the original data is directly used for modeling without pre-processing, the model's accuracy is highly reduced. The necessary data pre-processing improves the accuracy of the estimation model. Through the adaptive data pre-processing method proposed in this paper, the original capacity data is smoothed and denoised, so the processed data has a steady trend of monotonic decline. The proposed SW-LSTM model is constructed to learn the degradation trend in early life to establish the estimation model, which is then introduced into the capacity estimation process to obtain accurate results. The estimation effects of the SW-LSTM and LSTM models are conducted and analyzed under different operating conditions to test the adaptive ability of the varying training and testing lengths. By conducting different starting time tests for the effect verification using different sliding window sizes, it is observed that the estimation model has the same adaptive ability except for sliding window size 10, which showed optimal results. Upon selecting a W10 as the optimal sliding window value, the degradation trend for the real-world dataset with good evaluation effects at different training and prediction cycles is shown in Figure 8.

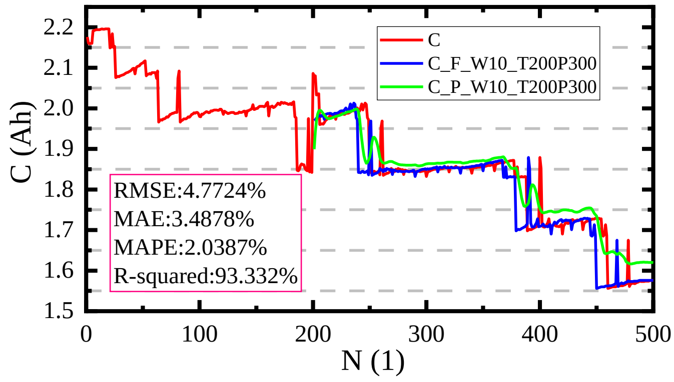

(a) Charging capacity estimation with W10_T200P300

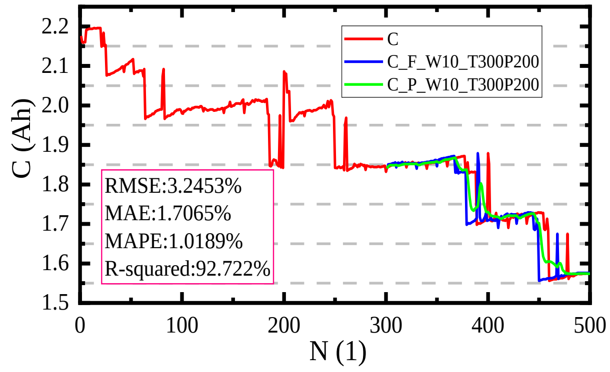

(b) Charging capacity estimation with W10_T300P200

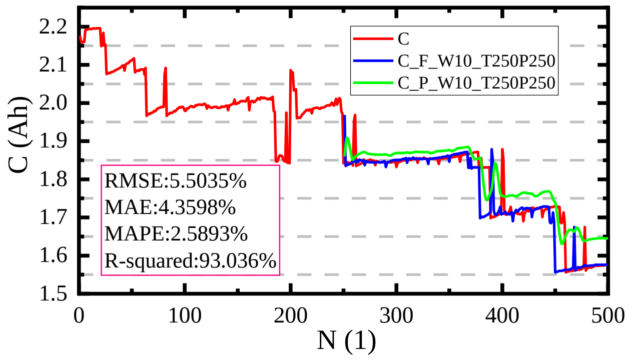

(c) Charging capacity estimation with W10_T250P250

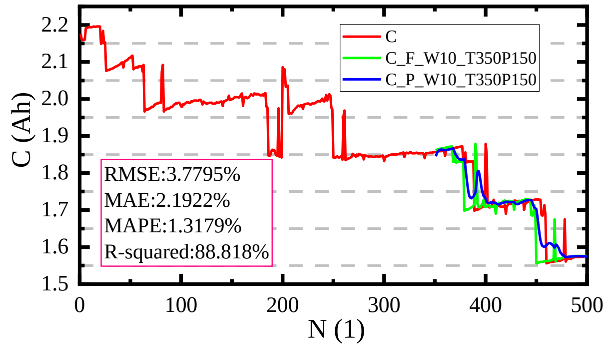

(d) Charging capacity estimation with W5_T350P150

Figure 8. Charging capacity estimation adaptive to varying training-testing datasets under the real-world BBDST working condition

In Figure , different conditions for the training and testing datasets are designed and realized with high accuracy. The blue and green lines represent the cycle-to-cycle capacity estimated by the SW-LSTM model. The estimation results are obtained for four types of datasets with four starting cycle-number points. It can be observed that when the battery's capacity is estimated by the proposed SW-LSTM model, the result fluctuates around the actual capacity curve, and there is only a slight difference between the two curves is slightly different under the two conditions. The estimation result has the same changing trend compared with the filtered capacity variation when using a window width of 10. To verify the estimation effect of the SW-LSTM model adapting to different starting points, the W10_T300P200, W10_T300P200, W10_T250P250, and

W5_T350P150 experiments are conducted. For different conditions, the predicted effect has a good estimation effect and a similar degradation trend to the original capacity fading trend. The results show that the estimation effect has an overall best RMSE value of 3.2453%, an MAE value of 1.7065%, a MAPE value of 1.018%, and an R-squared value of 92.72%. These estimation results demonstrate how adaptable and accurate the SW-LSTM model is for estimating lithium-ion battery capacity. The final comparative performance results using the RMSE, MAE, MAPE, and R-squared for the results presented in Figure 8 are shown in Figure 9.

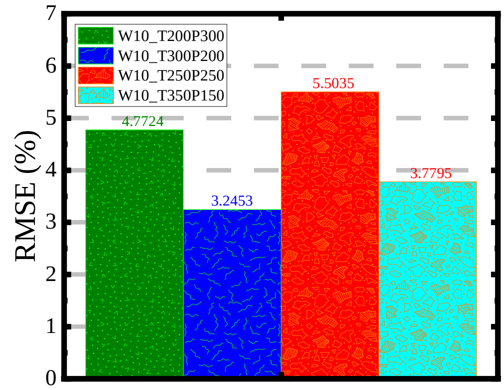

(a) RMSE histogram

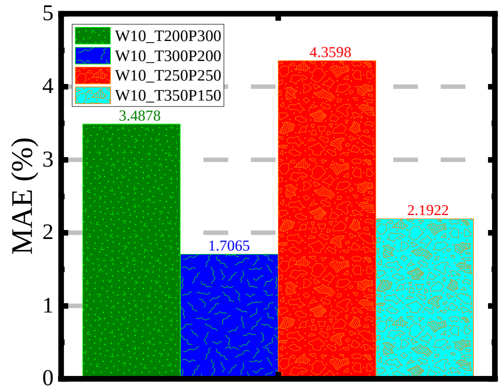

(b) MAE histogram

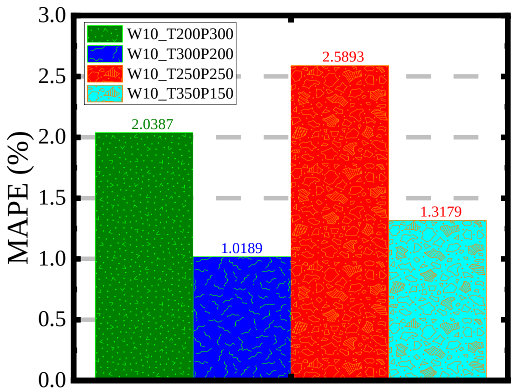

(c) MAPE histogram

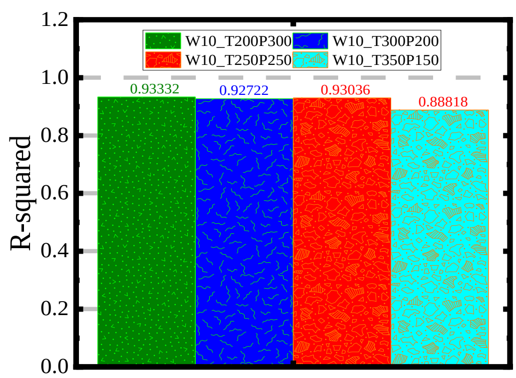

(d) R-squared histogram

Figure 9. Evaluation metric curves for different training and prediction cyclic capacity estimation

In Figure 9, comparing the values of the various metrics, it can be observed that, using a sliding window size of 10, the values are highly optimal for real-time application under conditions with different training and prediction cycles. Using a sliding window of W10 for different training and prediction cyclic capacity estimations, the proposed SW-LSTM model shows results with overall best RMSE, MAE, MAPE, and R-squared values of 3.2453%, 1.7065%, 1.0189%, and 92.722%, respectively, exhibiting high robustness for real-world capacity estimation of lithium-ion batteries.

3.4 *Comparison of the proposed model with other existing methods*

In this section, the estimation performance of the proposed model is compared with that of other machine learning methods, such as deep transfer convolutional neural network (DTCNN), Fiber Bragg Grating-Gaussian Process Regression (FBG-GPR), and sine cosine algorithm-salp swarm algorithm-extreme learning machine (SCA-SSA-ELM), using the MAE, RMSE, MAPE, and R-squared to verify the model's superiority and demonstrate the indispensable contribution, as shown in Table 1.

Table 1. Comparison of the proposed SW-LSTM with other existing methods

Methods	MAE	RMSE	MAPE	R-squared
DTCNN [62]	-	2.20%	2.47%	-
FBG-GPR [63]	1.02%	0.62%	-	-
SCA-SSA-ELM [64]	0.538%	1.156%	0.887%	99.98%
HFCM-LSTM [65]	0.46%	0.91%	-	-
Proposed SW-LSTM	0.019656%	0.033242%	1.1833%	92.08%

It can be observed from Table 1 that the capacity estimated by the proposed SW-LSTM model is optimally compared to the other existing methods using the same metrics as the reference value, which indicates that the proposed SW-LSTM model has high levels of robustness and low error. The findings of the current study and a few pertinent, recently published research studies are summarized in Table 1, which makes it clear that the proposed SW-LSTM prediction model offers good prediction accuracy over an extended period. This also serves as further evidence that the SW-LSTM model has distinct advantages in estimating lithium-ion battery capacity and has a strong capacity for generalization in real-world conditions.

4. Conclusion

Efficient and accurate capacity estimation plays an important role in battery health management. To overcome the difficulties with accurate capacity estimation, the improved SW-LSTM model is constructed by considering multiple time scale factors, in which the convolutional calculation and data distribution model are optimized by constructing an optimal DI-MAA model, thus building a DL network with both speed and accuracy for high-precision capacity estimation only using the high-randomness charging characteristics. The typical dynamic time is expanded statically to obtain the complete characteristics of time and space as two-dimensional information, forming a strong adaptive estimation algorithm combined with iterative optimization exploration. In the experimental verification process, the maximum capacity estimation error is 3.56%, and the average relative error is 0.032 under the complex real-world BBDST working conditions when only taking the rich-noise charging dataset as input. It has high accuracy, reduces estimation error, and has good stability, which provides a reference for the capacity estimation research of lithium-ion batteries. The proposed SW-LSTM estimation model deeply analyzes the battery characteristics by revealing the modeling and optimization mechanisms with the DI-MAA dataset pre-processing strategies. Consequently, a robust cycle life estimation model that is adaptive to complex working conditions has been established, which lays the theoretical foundation for the industrial application and promotion of lithium-ion batteries.

Acknowledgments

The work is supported by the National Natural Science Foundation of China (No. 62173281, 61801407), the Natural Science Foundation of Southwest University of Science and Technology (No. 17zx7110, 18zx7145), the Robot Technology used for the Special Environment Key Laboratory Fund of Sichuan Province (No. 18kftk03), and Robert Gorden University.

Competing Interests

The authors declare no Competing Financial or Non-Financial Interests.

Author Contribution

Shunli Wang: Conceptualization, methodology, and software.

Paul Takyi-Aninakwa: Software and validation.

Siyu Jin: Visualization and investigation.

Ke Liu: Data curation, writing, and original draft preparation.

Carlos Fernandez: Writing-reviewing and editing.

Data Availability

All data included in this study are available upon request by contact with the corresponding author.

References

1. Ran, A., et al., *Fast Remaining Capacity Estimation for Lithium-ion Batteries Based on Short-time Pulse Test and Gaussian Process Regression.* Energy & Environmental Materials, 2022.
2. Takyi-Aninakwa, P., et al., *An optimized relevant long short-term memory-squared gain extended Kalman filter for the state of charge estimation of lithium-ion batteries.* Energy, 2022. **260**: p. 1-15.
3. Tian, J., et al., *Data-driven battery degradation prediction: Forecasting voltage-capacity curves using one-cycle data.* EcoMat, 2022. **4**(5).
4. Ran, A., et al., *Fast Clustering of Retired Lithium-ion Batteries for Secondary Life with A Two-step Learning Method.* ACS Energy Lett., 2022. **7**(11): p. 3817–3825.
5. Takyi-Aninakwa, P., et al., *An optimized long short-term memory-weighted fading extended Kalman filtering model with wide temperature adaptation for the state of charge estimation of lithium-ion batteries.* Applied Energy, 2022. **326**.
6. Wang, S., et al., *An improved feedforward-long short-term memory modeling method for the whole-life-cycle state of charge prediction of lithium-ion batteries considering current-voltage-temperature variation.* Energy, 2022. **254**.
7. Takyi-Aninakwa, P., et al., *A strong tracking adaptive fading-extended Kalman filter for the state of charge estimation of lithium-ion batteries.* International Journal of Energy Research, 2022.
8. Tian, J., et al., *Battery state-of-charge estimation amid dynamic usage with physics-informed deep learning.* Energy Storage Materials, 2022. **50**: p. 718-729.
9. Zhang, Y., et al., *Weight optimized unscented Kalman filter for degradation trend prediction of lithium-ion battery with error compensation strategy.* Energy, 2022. **251**: p. 1-12.
10. Tong, Z., et al., *Early prediction of remaining useful life for Lithium-ion batteries based on a hybrid machine learning method.* Journal of Cleaner Production, 2021. **317**: p. 1-13.
11. Hannan, M.A., et al., *A review of lithium-ion battery state of charge estimation and management system in electric vehicle applications: Challenges and recommendations.* Renewable and Sustainable Energy Reviews, 2017. **78**: p. 834-854.
12. Wu, X., et al., *Progress, Key Issues, and Future Prospects for Li-Ion Battery Recycling.* Glob Chall, 2022. **6**(12): p. 2200067.
13. Xiang, S., et al., *Automatic multi-differential deep learning and its application to machine remaining useful life prediction.* Reliability Engineering & System Safety, 2022. **223**: p. 1-12.
14. Xia, P., et al., *Fault Knowledge Transfer Assisted Ensemble Method for Remaining Useful Life Prediction.* IEEE Transactions on Industrial Electronics, 2022. **18**(3): p. 1758-1769.
15. Wang, C., et al., *A novel long short-term memory networks-based data-driven prognostic strategy for proton exchange membrane fuel cells.* International Journal of Hydrogen Energy, 2022. **47**(18): p. 10395-10408.
16. Song, Y., et al., *A hybrid statistical data-driven method for on-line joint state estimation of lithium-ion batteries.* Applied Energy, 2020. **261**.
17. Cheng, M., et al., *A sustainable framework for the second-life battery ecosystem based on blockchain.* eTransportation, 2022. **14**.
18. Wang, S., et al., *A novel charged state prediction method of the lithium ion battery packs based on the composite equivalent modeling and improved splice Kalman filtering algorithm.* Journal of Power Sources, 2020. **471**.
19. Zhang, Q., et al., *A deep learning method for lithium-ion battery remaining useful life prediction based on sparse segment data via cloud computing system.* Energy, 2022. **241**: p. 1-11.
20. Li, P., et al., *An end-to-end neural network framework for state-of-health estimation and remaining useful life prediction of electric vehicle lithium batteries.* Renewable & Sustainable Energy Reviews, 2022. **156**: p. 1-12.
21. Ma, G., et al., *Remaining useful life prediction of lithium-ion batteries based on false nearest neighbors and a hybrid neural network.* Applied Energy, 2019. **253**.
22. Li, P., et al., *State-of-health estimation and remaining useful life prediction for the lithium-ion battery based on a variant long short term memory neural network.* Journal of Power Sources, 2020. **459**.

23. Gong, Y., et al., *State-of-health estimation of lithium-ion batteries based on improved long short-term memory algorithm.* Journal of Energy Storage, 2022. **53**.
24. Xiao, F., et al., *State of charge estimation for lithium-ion battery based on Gaussian process regression with deep recurrent kernel.* International Journal of Electrical Power & Energy Systems, 2021. **124**.
25. Yang, H., et al., *Remaining useful life prediction based on denoising technique and deep neural network for lithium-ion capacitors.* eTransportation, 2020. **5**.
26. Zhang, Y., et al., *State-of-health estimation for lithium-ion batteries by combining model-based incremental capacity analysis with support vector regression.* Energy, 2022. **239**.
27. Shen, D., et al., *A novel online method for predicting the remaining useful life of lithium-ion batteries considering random variable discharge current.* Energy, 2021. **218**.
28. Zhang, Z., et al., *Remaining useful life prediction of lithium-ion batteries based on attention mechanism and bidirectional long short-term memory network.* Measurement, 2022. **204**.
29. Ungurean, L., M.V. Micea, and G. Carstoiu, *Online state of health prediction method for lithium-ion batteries based on gated recurrent unit neural networks.* International Journal of Energy Research, 2020. **44**(8): p. 6767-6777.
30. Hesabi, H., M. Nourelfath, and A. Hajji, *A deep learning predictive model for selective maintenance optimization.* Reliability Engineering & System Safety, 2022. **219**: p. 1-10.
31. Román-Ramírez, L.A. and J. Marco, *Design of experiments applied to lithium-ion batteries: A literature review.* Applied Energy, 2022. **320**.
32. Ye, Z. and J. Yu, *State-of-Health Estimation for Lithium-Ion Batteries Using Domain Adversarial Transfer Learning.* IEEE Transactions on Power Electronics, 2022. **37**(3): p. 3528-3543.
33. Shen, S., et al., *A deep learning method for online capacity estimation of lithium-ion batteries.* Journal of Energy Storage, 2019. **25**: p. 1-13.
34. Wang, Y., et al., *A review of key issues for control and management in battery and ultra-capacitor hybrid energy storage systems.* eTransportation, 2020. **4**.
35. Qiu, R.J., et al., *Energy models and the process of fluid-magnetic separation for recovering cobalt micro-particles from vacuum reduction products of spent lithium ion batteries.* Journal of Cleaner Production, 2021. **279**.
36. Xu, C., et al., *Experimental study on thermal runaway propagation of lithium-ion battery modules with different parallel-series hybrid connections.* Journal of Cleaner Production, 2021. **284**(124749): p. 1-13.
37. Tian, J.Q., Y.J. Wang, and Z.H. Chen, *An improved single particle model for lithium-ion batteries based on main stress factor compensation.* Journal of Cleaner Production, 2021. **278**(123456): p. 1-12.
38. Oyewole, I., A. Chehade, and Y. Kim, *A controllable deep transfer learning network with multiple domain adaptation for battery state-of-charge estimation.* Applied Energy, 2022. **312**.
39. Wang, F.K., et al., *A hybrid method for online cycle life prediction of lithium-ion batteries.* International Journal of Energy Research, 2022. **46**(7): p. 9080-9096.
40. Jiang, B., et al., *A comparative study of different features extracted from electrochemical impedance spectroscopy in state of health estimation for lithium-ion batteries.* Applied Energy, 2022. **322**.
41. Sui, X., et al., *A review of non-probabilistic machine learning-based state of health estimation techniques for Lithium-ion battery.* Applied Energy, 2021. **300**.
42. Tan, X., et al., *Intelligent Online Health Estimation for Lithium-Ion Batteries Based on a Parallel Attention Network Combining Multivariate Time Series.* Frontiers in Energy Research, 2022. **10**: p. 1-12.
43. Wang, Z., N. Liu, and Y. Guo, *Adaptive sliding window LSTM NN based RUL prediction for lithium-ion batteries integrating LTSA feature reconstruction.* Neurocomputing, 2021. **466**: p. 178-189.
44. Zhang, Y., et al., *Long Short-Term Memory Recurrent Neural Network for Remaining Useful Life Prediction of Lithium-Ion Batteries.* IEEE Transactions on Vehicular Technology, 2018. **67**(7): p. 5695-5705.
45. Zhang, W., X. Li, and X. Li, *Deep learning-based prognostic approach for lithium-ion batteries with adaptive time-series prediction and on-line validation.* Measurement, 2020. **164**: p. 1-14.
46. Ardeshiri, R.R., M. Liu, and C. Ma, *Multivariate stacked bidirectional long short term memory for lithium-ion battery health management.* Reliability Engineering & System Safety, 2022. **224**(2): p. 1-19.

47. Chen, J., et al., *SOC estimation for lithium-ion battery using the LSTM-RNN with extended input and constrained output.* Energy, 2023. **262**.
48. Zuo, J., et al., *Deep learning based prognostic framework towards proton exchange membrane fuel cell for automotive application.* Applied Energy, 2021. **281**: p. 1-13.
49. Ma, J., et al., *Cycle life test optimization for different Li-ion power battery formulations using a hybrid remaining-useful-life prediction method.* Applied Energy, 2020. **262**: p. 1-16.
50. Elizabeth Michael, N., et al., *Short-term solar irradiance forecasting based on a novel Bayesian optimized deep Long Short-Term Memory neural network.* Applied Energy, 2022. **324**.
51. Li, S., et al., *Health-Conscious vehicle battery state estimation based on deep transfer learning.* Applied Energy, 2022. **316**: p. 1-8.
52. Luo, K., et al., *A review of deep learning approach to predicting the state of health and state of charge of lithium-ion batteries.* Journal of Energy Chemistry, 2022. **74**: p. 159-173.
53. Hong, J., et al., *Towards the swift prediction of the remaining useful life of lithium-ion batteries with end-to-end deep learning.* Applied Energy, 2020. **278**: p. 1-12.
54. Nascimento, R.G., et al., *Hybrid physics-informed neural networks for lithium-ion battery modeling and prognosis.* Journal of Power Sources, 2021. **513**: p. 1-13.
55. Ma, J., et al., *A hybrid transfer learning scheme for remaining useful life prediction and cycle life test optimization of different formulation Li-ion power batteries.* Applied Energy, 2021. **282**: p. 1-17.
56. Li, W., et al., *One-shot battery degradation trajectory prediction with deep learning.* Journal of Power Sources, 2021. **506**: p. 1-11.
57. Kim, S., et al., *Forecasting state-of-health of lithium-ion batteries using variational long short-term memory with transfer learning.* Journal of Energy Storage, 2021. **41**: p. 1-9.
58. Hu, X., et al., *Research directions for next-generation battery management solutions in automotive applications.* Renewable & Sustainable Energy Reviews, 2021. **152**: p. 1-14.
59. Hossain Lipu, M.S., et al., *Data-driven state of charge estimation of lithium-ion batteries: Algorithms, implementation factors, limitations and future trends.* Journal of Cleaner Production, 2020. **277**.
60. Bian, C., et al., *State-of-charge sequence estimation of lithium-ion battery based on bidirectional long short-term memory encoder-decoder architecture.* Journal of Power Sources, 2020. **449**.
61. Tian, Y., et al., *A combined method for state-of-charge estimation for lithium-ion batteries using a long short-term memory network and an adaptive cubature Kalman filter.* Applied Energy, 2020. **265**.
62. Yao, J. and T. Han, *Data-driven lithium-ion batteries capacity estimation based on deep transfer learning using partial segment of charging/discharging data.* Energy, 2023. **271**.
63. Li, Y., et al., *A hybrid machine learning framework for joint SOC and SOH estimation of lithium-ion batteries assisted with fiber sensor measurements.* Applied Energy, 2022. **325**.
64. Almaita, E., et al., *State of charge estimation for a group of lithium-ion batteries using long short-term memory neural network.* Journal of Energy Storage, 2022. **52**.
65. Gao, M., et al., *HFCM-LSTM: A novel hybrid framework for state-of-health estimation of lithium-ion battery.* Energy Reports, 2023. **9**: p. 2577-2590.